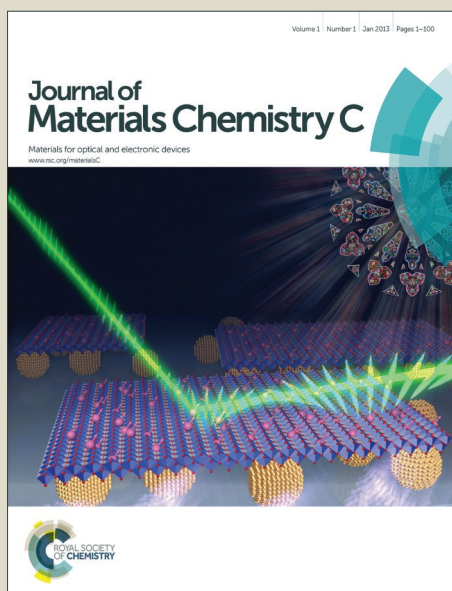


# Journal of Materials Chemistry C

Accepted Manuscript



This is an *Accepted Manuscript*, which has been through the Royal Society of Chemistry peer review process and has been accepted for publication.

*Accepted Manuscripts* are published online shortly after acceptance, before technical editing, formatting and proof reading. Using this free service, authors can make their results available to the community, in citable form, before we publish the edited article. We will replace this *Accepted Manuscript* with the edited and formatted *Advance Article* as soon as it is available.

You can find more information about *Accepted Manuscripts* in the [Information for Authors](#).

Please note that technical editing may introduce minor changes to the text and/or graphics, which may alter content. The journal's standard [Terms & Conditions](#) and the [Ethical guidelines](#) still apply. In no event shall the Royal Society of Chemistry be held responsible for any errors or omissions in this *Accepted Manuscript* or any consequences arising from the use of any information it contains.



Journal Name

ARTICLE

## An Organic-Inorganic Hybrid Co-crystal Complex as High-Performance Solid-State Nonlinear Optical Switch

Tianliang Chen, Zhihua Sun,\* Sangen Zhao, Chengmin Ji and Junhua Luo\*

Received 00th January 20xx,  
Accepted 00th January 20xx

DOI: 10.1039/x0xx00000x

www.rsc.org/

Solid state nonlinear optical (NLO) switches have attracted great interest, while high performance solid-state nonlinear optical (NLO) switches still remain scarce. Here, we firstly present a high-performance solid-state NLO switch based on an organic-inorganic hybrid co-crystal complex,  $[H_2dabcoCl_2][FeCl_3(H_2O)_3]$  (**1**, dabco = 1,4-diazabicyclo[2.2.2]octane). It is found that **1** exhibits a moderately large NLO response of  $\sim 0.31 \text{ pm} \cdot \text{V}^{-1}$ , superior switching-contrast ( $\sim 25$ ) and highly tunable repeatability, which may guarantee its potential device application. In addition, the microscopic crystal structural analyses reveal that its NLO switching is attributed to the order-disorder transformation of the dabco cation, cooperated with the reorientational displacement of the inorganic  $[FeCl_3(H_2O)_3]$  component. Owing to the broader designability of organic-inorganic hybrids, this work opens up an attractive approach for exploring new high-performance NLO switches.

### Introduction

Controllable and switchable nonlinear optical (NLO) materials are those that can reversibly change NLO efficiencies to enable responses to external stimuli, such as temperature, light, press, electric and magnetic fields, *etc.*<sup>[1]</sup> In comparison with the switching of third-order NLO properties in solutions,<sup>[2]</sup> the solid-state NLO switches are more promising because their macroscopic NLO properties can be modulated at bulk scale.<sup>[3]</sup> However, the exploration for high-performance solid-state NLO switches remains a challenge. The first example of switching second-harmonic generation (SHG) properties in bulk sample was demonstrated in the poled azobenzene and spirogyra-containing polymers.<sup>[3a]</sup> Nevertheless, the thermally randomization of chromophores leads to an irreversible decay of the NLO properties and eventually to a centrosymmetric structure. After that, the photochromic crystals and thin films of ruthenium complexes (based on redox switching) were used as classic examples to design solid-state NLO switches.<sup>[3c-3d]</sup> However, their NLO contrasts reported have fallen into a low value of 1.3-10 and only a limited number of "on/off" cycles were obtained. Recently, a more appealing approach of switching NLO response of compounds is a reversible phase transition (PT) from the non-centrosymmetric (NCS) to centrosymmetric (CS) order. Using this conceptually new scheme, a few solid-state NLO switches of simple organic salts and metal-organic frameworks have been reported.<sup>[4]</sup> They

usually exhibit the macroscopic NLO response between 0.05 and  $0.3 \text{ pm} \cdot \text{V}^{-1}$ , and the high-performance NLO switches with relatively large optical nonlinearities are still very sparse. In this context, it is highly-desirable to explore new and high-performance solid state NLO switches.

Recently, as one of the most promising strategies, co-crystals have received a great deal of attentions as a means of modifying the properties of compounds (NLO, ferroelectric and stability, *etc.*) by the synergistic effects of the individual components.<sup>[5]</sup> Among them, the organic-inorganic hybrid co-crystal has been highlighted more potential due to the possibility of combining desirable organic and inorganic characteristics within a single molecular scale composite.<sup>[6]</sup> However, it has been never reported to utilize this promising scheme to design the high-performance NLO switches based on PT up to now. Lately, the simple organic salts based on the flexible unit have been pioneered to be used to construct the structural phase transition materials due to the rotations of the flexible molecule in the crystal lattices.<sup>[7]</sup> From this point of view, 1,4-diazabicyclo[2.2.2]octane (dabco), a highly symmetric tertiary diamine with a globular shape, will undergo the dynamic motions under external stimuli. Such a structural feature is favorable to the occurrence of phase transition, as well as the generation of NLO effects. In addition, the inorganic phase transition compounds are usually associated with atomic displacement.<sup>[8]</sup> The well-known representative is  $\text{BiTiO}_3$ , of which the transition is triggered by the  $\text{Ti}^{4+}$  atom along the *c*-axis.<sup>[8a]</sup> When combining the flexible organic component with the simple neutral inorganic component by hydrogen bonds or by other non-covalent bonds, it will construct an organic-inorganic hybrid co-crystal complex. Such co-crystal systems have been proved to be readily able to undergo transformations with the breaking of the crystallographic symmetry.<sup>[9]</sup> Moreover, due to the strength

Key Laboratory of Optoelectronic Materials Chemistry and Physics, Fujian Institute of Research on the Structure of Matter, Chinese Academy of Sciences, Fuzhou, 350002, P. R. China.

\*To whom correspondence should be addressed: E-mail: [sunzhihua@fjirsm.ac.cn](mailto:sunzhihua@fjirsm.ac.cn) and [jlhlo@fjirsm.ac.cn](mailto:jlhlo@fjirsm.ac.cn); Fax: (+86) 591-83730955; Tel: (+86) 591-83730955. Electronic Supplementary Information (ESI) available: bulk crystal, crystal data, PXRD, See DOI: 10.1039/x0xx00000x

and directionality of hydrogen bonds, the origin of their PT can be roughly ascribed to the strong coupling motions of atoms or polar components in the crystal lattices, such as order-disorder movement of flexible molecules and reorientational displacements of inorganic component.<sup>[9]</sup> It can be expected that these strong couplings may induce the large molecular moments and thus lead to large macroscopic NLO response in the SHG-ON state when the phase transition is from NC order to NCS order.

In this work, we present a high-performance NLO switch based on an organic-inorganic hybrid co-crystal complex, 1,4-diazabicyclo[2.2.2]octane (dabco), [H<sub>2</sub>dabcoCl<sub>2</sub>][FeCl<sub>3</sub>(H<sub>2</sub>O)<sub>3</sub>] (**1**). **1** exhibits a moderately large NLO response of 0.31 pm·V<sup>-1</sup>, superior switching-contrast (~25) and remarkable switching reversibility, which is triggered by the coupling of the order-disorder transformation of the organic dabco cation and the reorientational displacements of the inorganic [FeCl<sub>3</sub>(H<sub>2</sub>O)<sub>3</sub>] component. These findings provide a novel promising strategy to design high-performance NLO switch materials.

## Experimental section

**Synthetic procedures.** All the starting materials were of analytical reagent grade and were used without further purification. Firstly, the dihydrochloride salts of triethylenediamine (dabco·2HCl) were prepared by mixing the solution of concentrated hydrochloric acid and dabco with a 3:1 molar ratio in water; Secondly, a filtered solution of iron (III) chloride (1 molar equiv) was put in above solution; Finally, the solution was filtered and kept for evaporation at room temperature for several days to obtain brown cubic crystal (Figure S1). The purity of co-crystal **1** was confirmed by its X-ray powder diffraction (PXRD) (Figure S2).

**Single-Crystal X-ray Crystallography.** Variable-temperature X-ray single crystal diffraction experiments were carried on SuperNova CCD diffractometer with the graphite monochromated Mo K $\alpha$  radiation ( $\lambda = 0.7 \text{ \AA}$ ) at 100 K and 290 K, respectively. Crystal Clear software package (Rigaku) was utilized for data collection, cell refinement and data reduction. Crystal structures were solved by the direct methods and refined by the full-matrix method based on  $F^2$  using the SHELXL97 software package.<sup>[10]</sup> Anisotropic thermal parameters were refined for the non-hydrogen atoms using all reflections. The positions of hydrogen atoms were generated geometrically. The asymmetric units and the packing diagrams were drawn with DIAMOND (Brandenburg and Putz, 2005). Distances and angles between some atoms were calculated using DIAMOND, while other calculations were carried out using SHELXL97. Table S1 shows the crystal data and structure refinement of **1**. CCDC 1058268 and CCDC 1058269 contain the supplementary crystallographic data for this paper. These data can be obtained free of charge from The Cambridge Crystallographic Data Centre via [www.ccdc.cam.ac.uk/data\\_request/cif](http://www.ccdc.cam.ac.uk/data_request/cif).

**DSC and Specific Heat Measurements.** Differential scanning calorimetry (DSC) at different scanning rate (10 K/min, 5 K/min and 2 K/min) and specific heat ( $C_p$ ) measurements were

carried out on a NETZSCH DSC 200 F3 instrument in the temperature range from 240 K to 290 K. The experiments were performed under nitrogen condition in aluminium crucibles.

**SHG Activities Measurements.** All of the NLO properties were measured using an Nd:YAG laser with an input pulse of 420 mV (pulsed at a wavelength of 1064 nm, 5 ns pulse duration, 1.6 MW peak power, 10 Hz repetition rate). SHG-switching experiments were performed on crystals in the range of 240–290 K. Compound **1** with sizes in the range of 25–210  $\mu\text{m}$ , sieved through a series of mesh, was utilized to perform phase-matching experiment at 160 K by the approximate model of Kurtz and Perry.<sup>[11]</sup> The measured SHG effects were compared with that of KH<sub>2</sub>PO<sub>4</sub> ( $\chi^{(2)} = 0.39 \text{ pm}\cdot\text{V}^{-1}$ ). The SHG switching contrast was defined as the ratio of SHG signals below and above phase transition point, respectively. In its CS state, the measured standard deviation of noise level was used as the denominator.<sup>[4b]</sup>

## Results and discussion

Compound **1** was prepared as orange bulk single crystals up to  $6 \times 6 \times 3 \text{ mm}^3$  by slow evaporation (Figure S1, Supporting Information). DSC and  $C_p$  measurements (Figure 1) indicate a structural phase transition of **1** at  $T_c = 279.9 \text{ K}$ . The corresponding enthalpy change  $\Delta S$  in the heating mode are estimated to be 0.663 J/mol·K from the  $C_p$ - $T$  curve. Given that Boltzmann equation of  $\Delta S = R \ln N$ , in which  $R$  is the gas constant and  $N$  is the ratio of numbers of respective geometrically distinguishable orientations,  $N = 1.94$  is obtained, showing a typical disorder-order feature of the phase transition.<sup>[12]</sup> To further confirm the type of phase transition, DSC measurement of **1** under different cooling/heating rates was performed.<sup>[13]</sup> As shown in Figure S3, when the heating/cooling rates were reduced to 2 K/min, the thermal hysteresis is 0.9 K. Such a narrow thermal hysteresis indicates a characteristic of the second-order phase transition.

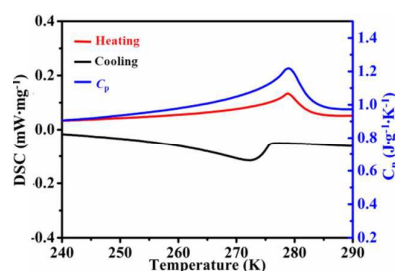


**Figure 1.** The temperature-dependent heat flow measurements: Differential calorimetric and specific heat measurements of powder samples of **1**.

Variable-temperature single-crystal structures of **1** were performed at 293 K (high-temperature phase, HTP) and 100 K (low-temperature phase, LTP), respectively. In HTP, **1** crystallizes in the orthorhombic crystal system,  $Pnma$  (NO, 62) and point group  $D_{2h}$ . The asymmetric unit of **1** contains one-half of organic dabcodihydrochloride (H<sub>2</sub>dabco·2Cl) species and one-half of inorganic [FeCl<sub>3</sub>(H<sub>2</sub>O)<sub>3</sub>] species (Figure 2a). The iron (III) ion adopts a distorted octahedral geometry in which

the apical atom is Cl1 anion, and the four equatorial atoms are O1, O2, O3 atoms and Cl2 anion, respectively. Due to the equatorial plane and the iron (III) atoms lying on a mirror plane, the inorganic  $[\text{FeCl}_3(\text{H}_2\text{O})_3]$  octahedron, which are connected into the inorganic layer by the hydrogen bonds  $\text{O}-\text{H}\cdots\text{Cl}_3$  (Figure 3a), can be generated from the unique atoms by the equatorial plane paralleled to  $ac$  plane (Figure 2a, Figure 3b, Figure S4). In addition, the corresponding angle of the equatorial plane of the neighbouring two  $[\text{FeCl}_3(\text{H}_2\text{O})_3]$  octahedrons is  $0^\circ$  (Figure S5). In inorganic layer, the distances of the nearest neighbouring Fe ions along  $c$ -axis and  $a$ -axis are 7.035 Å and 6.933 Å, respectively (Figure 3a). Furthermore, the adjacent inorganic layers are interlinked *via* the bifurcated hydrogen bonds  $\text{N1}-\text{H1}\cdots\text{Cl}$  provided by the dabco cations (Figure 2a). The dabco cations coincide with the inversion center of the unit cell, in which the C atoms are distributed between two positions related with a refined site occupancy factor equal to 0.5.

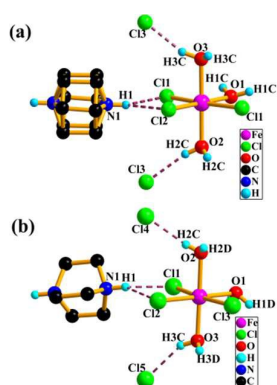


**Figure 2.** a) Asymmetric unit of **1** at 293 K; b) Asymmetric unit of **1** at 100 K. Hydrogen atoms on carbon atoms are omitted for clarity.

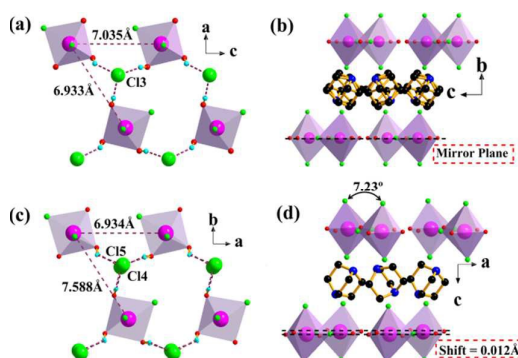


**Figure 3.** a) The inorganic layer of **1** in ( $a, c$ ) plane at 293 K, where the  $[\text{FeCl}_3(\text{H}_2\text{O})_3]$  octahedrons were linked by the two symmetry-equivalent trifurcated H-bond  $\text{O}-\text{H}\cdots\text{Cl}_3$ . The distances of the nearest neighbour Fe ions along  $c$ -axis and  $a$ -axis are 7.035 Å and 6.933 Å, respectively; b) An alternating inorganic-organic layered structure of **1** at 293 K; c) The inorganic layer of **1** in ( $a, b$ ) plane at 100 K, where the  $[\text{FeCl}_3(\text{H}_2\text{O})_3]$  octahedrons were linked by the two different trifurcated H-bond  $\text{O}-\text{H}\cdots\text{Cl}_4$  and  $\text{O}-\text{H}\cdots\text{Cl}_5$ . The distances of the nearest neighbour Fe ions along  $a$ -axis and  $b$ -axis are 6.934 Å and 7.588 Å, respectively; d) an alternating inorganic-organic layered structure of **1** at 100 K.

In the LTP, **1** still belongs to orthorhombic crystal system, but its symmetry is refined in space group  $P2_12_12_1$  (NO, 19) and point group  $D_2$ . The relationship between the two

temperature cells is  $a^{293\text{ K}} \approx b^{100\text{ K}}$ ,  $b^{293\text{ K}} \approx c^{100\text{ K}}$ ,  $c^{293\text{ K}} \approx b^{100\text{ K}}$ . The asymmetric unit contains one organic  $\text{H}_2\text{dabco}\cdot 2\text{Cl}$  species and one inorganic  $[\text{FeCl}_3(\text{H}_2\text{O})_3]$  species (Figure 2b). The Fe (III) ion still adopts a distorted octahedral geometry, in which the bond lengths (of Fe-Cl and Fe-O) and bond angles (Cl-Fe-O and O-Fe-O) exhibit just a little difference within 0.009 Å and  $1.12^\circ$ , compared to those in HTP (Table S2 and Table S3). However, the Fe ions are delocalized from the mirror plane with the deviation value 0.012 Å along  $c$ -axis (Figure 3d), leading to the disappearance of the mirror plane in the inorganic layer. At the same time, the angle of the equatorial plane of the neighboring  $[\text{FeCl}_3(\text{H}_2\text{O})_3]$  octahedron changes into  $7.23^\circ$  (Figure 3d and Figure S5), indicating that there exists a remarkable reorientation in the  $[\text{FeCl}_3(\text{H}_2\text{O})_3]$  octahedron. In inorganic layer, the corresponding distances of the nearest neighbouring Fe ions change into 6.934 Å and 7.588 Å (Figure 3c), suggesting that there are the evidently cooperative displacements between the Fe ions. Beside the pronounced change in the inorganic species, another dramatic difference occurs in the cationic part. That is, the disordered cations dabco become completely ordered and the carbon atoms can be determined into exclusive atomic positions when the temperature decreases to 100 K (Figure 2b and Figure 3d). Therefore, considering the ordering of dabco cation and the reorientation of the octahedron  $[\text{FeCl}_3(\text{H}_2\text{O})_3]$  accompanying with the collective relative displacements of the Fe atoms in LTP, it can be proposed that the order-disorder transition of dabco cation cooperated with the reorientational displacement of the octahedron  $[\text{FeCl}_3(\text{H}_2\text{O})_3]$  may be the driving force of the structural phase transition in such a co-crystal complex.<sup>[4e]</sup>

From the viewpoint of symmetry breaking, the HTP crystallizes in the centrosymmetric point group  $mmm$  and the LTP in a chiral point group 222. Namely, a symmetry breaking phenomenon occurs during the transition process with the symmetric elements decreasing by half from eight ( $E, i, \sigma_h, \sigma_v, \sigma_v', C_2, C_2', C_2''$ ) to four ( $E, C_2, \sigma_v, \sigma_v'$ ), which is in good agreement with Landau phase transition theory (Figure 4).<sup>[14]</sup> Furthermore, the symmetry breaking from CS phase to NCS phase can be also confirmed by the following temperature-dependent SHG experiments.

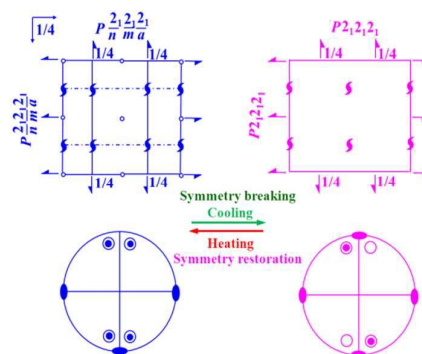


**Figure 4.** Symmetry breaking in **1** during its phase transition from HTP ( $Pnma$ , NO, 62) to LTP ( $P2_12_12_1$ , NO, 19)

An effective quadratic NLO switch is often associated with its SHG coefficient, switching contrast and reversible switching

cycles, etc. The absorption spectrum reveals that **1** has a wide transmission range from 500-1800 nm with an absorption edge of 425 nm, which might be caused by the absorption of  $\text{Fe}^{3+}$  ions. Such a result indicates that **1** is suitable for NLO application under the Nd:YAG laser ( $\lambda = 1064$  nm). Here, these SHG-switching performances of **1** were investigated in details. A study of temperature dependence of the SHG signal has been presented in Figure 5a. Above  $T_c$ , the SHG signal is absolutely negligible, treated as its switch-off state. While, the appearance of its SHG signal in the vicinity of the phase transition temperature reveals that **1** enters into its switch-on state, which is in good accordance with the structure change from CS phase to NCS phase. Additionally, it is clearly shown that the SHG signal is gradually amplified in intensity and approached almost saturation with the temperature decreasing from  $T_c$  to 160 K, suggesting a second-order phase transition feature, which is in well agreement with the aforementioned thermal analyses.

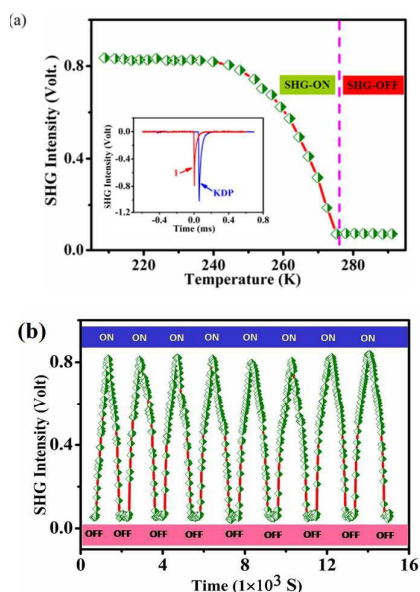


**Figure 5.** a) Temperature-dependent variation of SHG signals of **1** in the vicinity of  $T_c$ . A superior switching contrast of  $\sim 25$  is achieved; b) The SHG "on/off" cycles in **1**. It can be repeated at least 8 times without any obvious fatigue.

In order to measure the relative value of the SHG efficiency of **1**, powdered KDP was selected as standard sample. The SHG intensity at a saturation value is estimated to be  $\sim 0.8$  times as large as that of KDP (Figure 5a); namely, the quadratic NLO coefficient of **1** is calculated to be  $0.31 \text{ pm}\cdot\text{V}^{-1}$  (KDP,  $0.39 \text{ pm}\cdot\text{V}^{-1}$ ). This value is larger than other solid-state NLO switches such as  $\text{NH}_2\text{-MIL-53(Al)}$  ( $\sim 0.05 \pm 0.02 \text{ pm}\cdot\text{V}^{-1}$ ),<sup>[4b]</sup> bis(imidazolium hydrochlorate) dihydrate 18-crown-6 ( $\sim 0.08 \text{ pm}\cdot\text{V}^{-1}$ )<sup>[4e]</sup> and comparable with that of  $\alpha\text{-(H}_3\text{N(CH}_2)_2\text{-S-(CH}_2)_2\text{NH}_3\text{)Bil}_5$  (about  $0.3 \text{ pm}\cdot\text{V}^{-1}$ ).<sup>[4a]</sup> Such a moderately large SHG coefficient will lead to an obvious quadratic NLO switch activity between SHG-ON and SHG-OFF state with the contrast to be approximately 25, which is higher than most of reported solid-state NLO switches ( $1.3\sim 20$ )<sup>[3c-3h]</sup> It is believed that the improved contrast value of

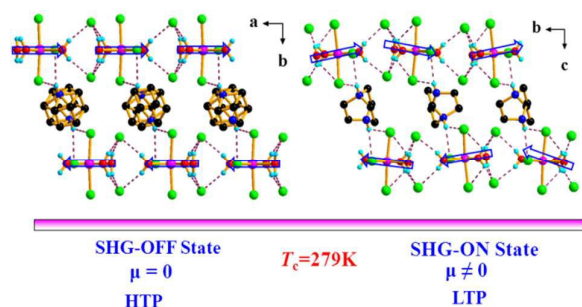
**1** would be obtained when the NLO switching experiment is performed along its phase-matchable direction.

Figure 5b shows that **1** exhibits a high repeatability of SHG switching with at least 8 cycles, which is much superior to many photochromic polymer films and photochromic crystals.<sup>[3c]</sup> Importantly, after a long time switching experiment, the intensities of its SHG signal still keeps its initial level without any obvious fatigue. As we all know, the NLO intensity is commonly relative to the arrangement of dipole in structure.<sup>[15]</sup> In poled polymers and redox-based switching LB films, the limitative number of "ON/OFF" cycles are possibly ascribed to their irreversible changes of initial chromophore alignment.<sup>[3]</sup> However, for **1**, the SHG switching scheme is established on its thermally induced structural change, which guarantees the molecular dipole moments to be reversibly tuned in a collective manner and results in the highly-reversible process.

Additionally, the phase-matchable experiments of **1** were performed using the Kurtz and Perry method. As expected, the intensity of **1** increases with particle size and approaches almost saturation with particle size up to  $200 \mu\text{m}$  (Figure S6) at 160 K, confirming the phase-matchable properties. All those findings indicate that **1** will possess the potential applications in SHG-switching.

In ionic crystal, the marked atomic displacements could induce the large molecular dipole moments, which may be closely relative to the macroscopic NLO response. Since the organic-inorganic hybrid co-crystal **1** is composed of one organic neutral component ( $\text{H}_2\text{dabco}\cdot 2\text{HCl}$ ) and one inorganic component ( $[\text{FeCl}_3(\text{H}_2\text{O})_3]$ ), its molecular dipole moments may be estimated from the synergistic effects of the molecular dipole moments of the individual components. In the "SHG-OFF" state, the C atoms and N atoms of organic dabco cation are distributed between two positions related by the centre of symmetry. Meanwhile, the inorganic  $[\text{FeCl}_3(\text{H}_2\text{O})_3]$  component are located on the mirror plane due to the symmetry requirement. Consequently, the molecular dipole moments of the organic  $\text{H}_2\text{dabco}\cdot 2\text{HCl}$  component and inorganic  $[\text{FeCl}_3(\text{H}_2\text{O})_3]$  component are cancelled out, resulting in the vanished SHG activity of **1** (shown in Figure 6(a)). However, in the "SHG-ON" state of LTP, the organic dabco cations are frozen to be ordered and all atoms can be exclusively determined, in which all of the atoms are crystallographically inequivalent. At the same time, a concomitant remarkable reorientational displacements occurs in inorganic  $[\text{FeCl}_3(\text{H}_2\text{O})_3]$  component. Accordingly, the Cl anions, Fe (III) centre ion, and N atoms are displaced from their equilibrium positions and the molecular dipole moments will be generated in the two individual components (Figures S7-S8). For the  $\text{H}_2\text{dabco}\cdot 2\text{HCl}$  species, N and Cl atoms were displaced from their equilibrium sites by a magnitude of  $-0.0046 \text{ \AA}$  and  $0.0096 \text{ \AA}$ , respectively. Furthermore, we assume that the dipole centres are located at the average protonated N of the dabco cation and the average two uncoordinated Cl atoms. The molecular dipole moment of the organic species was calculated to be

$0.716 \times 10^{-29}$  C·m; for the inorganic  $[\text{FeCl}_3(\text{H}_2\text{O})_3]$  component, due to the more pronounced deviation of the Fe (III) ion and  $\text{Cl}_2$  ion from their equilibrium sites ( $-0.0061 \times |\mathbf{b}|$  and  $-0.1428 \times |\mathbf{b}|$ , respectively), larger molecular dipole moments of the inorganic species are obtained ( $-11.1 \times 10^{-29}$  C·m). Finally, a large molecular dipole moment of **1** was achieved ( $-10.3 \times 10^{-29}$  C·m), resulting in a relatively large SHG signal (Figure 6b). Hence, the SHG switching of **1** may be assigned to the ionic displacements, triggered by organic cationic orderings coupled with reorientation displacements of inorganic  $[\text{FeCl}_3(\text{H}_2\text{O})_3]$  sheet.



**Figure 6.** Schematic diagram for the generation of molecular dipole moments in **1** during its SHG switching process. The highly disordering of the dabco cations lead to the loss of NLO activity in the RTP. The outline arrows denote the reorientation of the inorganic part  $[\text{FeCl}_3(\text{H}_2\text{O})_3]\text{Cl}_2$  in the SHG-ON state.

## Conclusions

In summary, a high-performance NLO switch based on an organic-inorganic hybrid co-crystal complex has been firstly reported. It exhibits an attractive NLO switching performance with a moderately large NLO response of  $\sim 0.31 \text{ pm}^2\text{V}^{-1}$ , a superior contrast of  $\sim 25$  and a highly-tunable repeatability, induced by the reversible solid-state phase transition. These results make **1** a promising material for the prospective NLO switch. Furthermore, the origin of NLO switching is induced by the coupling of the order-disorder transformation of organic cation and reorientational displacements of inorganic  $[\text{FeCl}_3(\text{H}_2\text{O})_3]$  component. Considering the structural diversity and tunability, inorganic-organic compounds afford abundant room for exploring new solid-state NLO switches. For instance, one can utilize  $\pi$ -conjugated charge-transfer dipoles to induce large molecular hyperpolarizability, as well as NLO effects. It is believed that such delicate chemical modifications will provide potentials to construct new high-performance NLO switches.

## Acknowledgements

This work was supported by NSFC (21222102, 21373220, 51402296, 21171166 and 21301172), the 973 Key Program of MOST (2011CB935904), the NSF for Distinguished Young Scholars of Fujian Province (2014J06015). Z.S. and S.Z. thanks the supports from "Chunmiao Projects" of Haixi Institute of

Chinese Academy of Sciences (CMZX-2013-002 and CMZX-2015-003).

## Notes and references

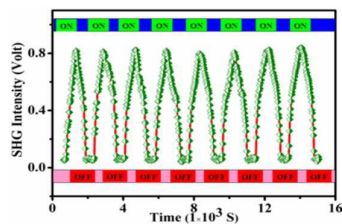
- 1 a) *Handbook of Stimuli-Responsive Materials* (Ed.: M.W. Urban), Wiley-VCH, Weinheim, **2011**; b) Y. Shi, C. Zhang, H. Zhang, J. Bechtel, L. Dalton, B. Robinson and W. Steier, *Science* **2000**, **288**, 119-122; c) M. Lee, H. E. Katz, C. Erben, D. M. Gill, P. Gopalan, J. D. Heber and D. J. McGee, *Science* **2002**, **298**, 1401-1403; d) F. Castet, V. Rodriguez, J.-L. Pozzo, L. Ducasse, A. Plaquet and B. Champagne, *Acc. Chem. Soc.*, **2013**, **46**, 2656-2665.
- 2 a) Z.-Y. Li and Z.-M. Meng, *J. Mater. Chem. C.*, **2014**, **2**, 783-800; b) Y. Liu, F. Qin, Z.-Y. Wei, Q.-B. Meng, D.-Z. Zhang and Z.-Y. Li, *Appl. Phys. Lett.*, **2009**, **95**, 131116; c) X. Hu, P. Jiang, C. Ding, H. Yang and Q. Gong, *Nature Photonics*, **2008**, **2**, 185-189.
- 3 a) K. Nakatani and J. A. Delaire, *Chem. Mater.*, **1997**, **9**, 2682-2684; b) M. Sliwa, S. Létard, I. Malfant, M. Nierlich, P. G. Lacroix, T. Asahi, H. Masuhara, P. Yu and K. Nakatani, *Chem. Mater.*, **2005**, **17**, 4727-4735; c) M. Sliwa, A. Spangenberg, I. Malfant, P. G. Lacroix, R. Métivier, R. B. Pansu, and K. Nakatani, *Chem. Mater.*, **2008**, **20**, 4062-4068; d) L. B.-Lecaque, B. J. Coe, K. Clays, S. Foerier, T. Verbiest and I. Asselberghs, *J. Am. Chem. Soc.*, **2008**, **130**, 3286-3287; e) P. Li, M.-S. Wang, M.-Jian. Zhang, C.-S. Lin, L.-Z. Cai, S. Guo and G.-C. Guo, *Angew. Chem. Int. Ed.*, **2014**, **53**, 11529-11531; f) J. Boixel, V. Guerschais, H. L. Bozec, D. Jacquemin, A. Amar, A. Boucekkine, A. Colombo, C. Dragonetti, D. Marinotto, D. Roberto, S. Righetto and R. D. Angelis, *J. Am. Chem. Soc.*, **2014**, **136**, 5367-5375; g) A. Priimagi, K. Ogawa, M. Virkki, J.-ichi Mamiya, M. Kauranen and A. Shishido, *Adv. Mater.*, **2012**, **24**, 6410-6415; h) S. L. Gilat, S. H. Kawai and J.-M. Lehn, *Chem. Eur. J.*, **1995**, **1**, 275-284; i) I. Asselberghs, Y. Zhao, K. Clays, A. Persoons, A. Comito and Y. Rubin, *Chem. Phys. Lett.*, **2002**, **364**, 279-283; j) F. Mançois, L. Sanguinet, J.-L. Pozzo, M. Guillaume, B. Champagne, V. Rodriguez, F. Adamietz, L. Ducasse and F. Castet, *J. Phys. Chem. B.*, **2007**, **111**, 9795-9802; k) A. Plaquet, M. Guillaume and B. Champagne, *J. Phys. Chem. C.*, **2008**, **112**, 5638-5645; l) E. Cariati, C. Dragonetti, E. Lucenti, F. Nisic, S. Righetto, D. Roberto and E. Tordin, *Chem. Commun.*, **2014**, **50**, 1608-1610.
- 4 a) W. Bi, N. Louvain, N. Mercier, J. Luc, I. Rau, F. Kajzar and B. Sahraoui, *Adv. Mater.*, **2008**, **20**, 1013-1017; b) P. Serra-Crespo, M. A. Van der Veen, E. Gobechiya, K. Houthoofd, Y. Filinchuk, C. E. A. Kirschhock, J. A. Martens, B. F. Sels, D. E. Vos, F. Kapteijn and J. Gascon, *J. Am. Chem. Soc.*, **2012**, **134**, 8314-8317; c) Z. Sun, J. Luo, S. Zhang, C. Ji, L. Zhou, S. Li, F. Deng and M. Hong, *Adv. Mater.*, **2013**, **25**, 4159-4163; d) C. Ji, Z. Sun, S. Zhang, S. Zhao, T. Chen, Y. Tang and J. Luo, *Chem. Commun.*, **2015**, **51**, 2298-2300; e) Z. Sun, S. Li, S. Zhang, F. Deng, M. Hong and J. Luo, *Adv. Optical Mater.*, **2014**, **2**, 1199-1205.
- 5 a) C. Bosshard, M. S. Wong, F. Pan, P. Günter, V. Gramlich, *Adv. Mater.*, **1997**, **9**, 554-557; b) S. Horiuchi, F. Ishii, R. Kumai, Y. Okimoto, H. Tachibana, N. Nagaosa and Y. Tokura, *Nat. Mater.*, **2005**, **4**, 163-166; c) T. Akutagawa, H. Koshinaka, D. Sato, S. Takeda, S.-I. Noro, H. Takahashi, R. Kumai, Y. Tokura and T. Nakamura, *Nat. Mater.*, **2009**, **8**, 342-347; d) O. Bolton and A. J. Matzger, *Angew. Chem. Int. Ed.*, **2011**, **50**, 8960-8963; e) Y.-Q. Sun, Y.-L. Lei, X.-H. Sun, S.-T. Lee and L.-S. Liao, *Chem. Mater.*, **2015**, **27**, 1157-1163; f) M. Dabros, P. R. Emery and V. R. Thalladi, *Angew. Chem. Int. Ed.*, **2007**, **119**, 4210-4213; g) J. Zhang,

- H. Geng, T. S. Virk, Y. Zhao, J. Tan and C. A. Di, *Adv. Mater.*, 2012, **24**, 2603–2607.
- 6 a) R. Saha, B. Joarder, A. S. Roy, S. M. Islam and S. Kumar, *Chem. Eur. J.*, 2013, **19**, 16607–16614; b) B. Dey, R. Saha and, P. Mukherjee, *Chem. Commun.*, 2013, **49**, 7064–7066; c) T. T. Ong, P. Kavuru, T. Nguyen, R. Cantwell, .Ł. Wojtas and M. J. Zaworotko, *J. Am. Chem. Soc.*, 2011, **133**, 9224–9227; d) G. Liu, J. Liu, Y. Liu and X. Tao, *J. Am. Chem. Soc.*, 2014, **136**, 590–593; e) R. Zhang, Q. Zhang, Z. Liu, L. Yang, J. Wu, H. Zhou, J. Yang and Y. Tian, *CrystEngComm*, 2014, **16**, 2039–2044.
- 7 a) D.-W. Fu, W. Zhang, H.-L. Cai, J.-Z. Ge, Y. Zhang and R.-G. Xiong, *Adv. Mater.*, 2011, **23**, 5658–5662; b) Z. Pająk, P. Czarnecki, B. Szafrńska, H. Małuszyńska and Z. Fojud, *J. Chem. Phys.*, 2006, **124**, 144502-1–6; c) M. Szafrąński, A. Katrusiak and G. J. McIntyre, *Phys. Rev. Lett.*, 2002, **89**, 215507:1-4; d) M. Szafrąński, *J. Phys. Chem. B*2011, **115**, 8755–8762; e) M. Węclawik, A. Gągor, A. Piecha, R. Jakubas and W. Medycki, *CrystEngComm.*, 2013, **15**, 5633–5640; f) X. Shi, J. Luo, Z. Sun, S. Li, C. Ji, L. Li, L. Han, S. Zhang, D. Yuan and M. Hong, *Cryst. Grow. Des.*, 2013, **13**, 2081–2086
- 8 a) H. D. Megaw, *Acta Cryst.*, 1952, **5**, 739-749; b) L. E. Cross and G. A. Rossetti, *J. Appl. Phys.*, 1991, **69**, 896–898; c) A. Katrusiak, *Phys. Rev. B.*, 1993, **48**, 2992-3002;
- 9 a) S. Yahyaoui, W. Rekić, H. Naïli, T. Mhiri and T. Bataille, *J. Solid State Chem.*, 2007, **180**, 3560–3570; b) H. Naïli, W. Rekić, T. Bataille and T. Mhirid, *Polyhedron.*, 2006, **25**, 3543–3554; c) J. Dolinšek, M. Klanjšek, D. Arčon, H. Kim, J. Seliger, V. Žagar and L. F. Kirpichnikova, *Phys. Rev. B.*, 1999, **59**, 3460-3467; d) G. V. Kozlov and A. A. Volkov, *Phys. Rev. B.*, 28, 255-261.
- 10 G. M. Sheldrick, *SHELXL-97*, University of Gottingen, Germany, 1997.
- 11 S. K. Kurtz and T. T. Perry, *J. Appl. Phys.* 1968, **39**, 3798-3813.
- 12 a) Z. Sun, S. Zhang, C. Ji, T. Chen and J. Luo, *J. Mater. Chem. C.*, 2014, **2**, 10337-10342; b) C. Ji, Z. Sun, S.-Q. Zhang, T. Chen, P. Zhou and J. Luo, *J. Mater. Chem. C.*, 2014, **2**, 567–572; c) P. Zhou, Z. Sun, S. Zhang, C. Ji, S. Zhao, R.-G. Xiong and J. Luo, *J. Mater. Chem. C.*, 2014, **2**, 2341-2345; d) H.-Y. Ye, S.-H. Li, Y. Zhang, L. Zhou, F. Deng and R.-G. Xiong, *J Am Chem. Soc.* 2014, **136**, 10033-10040.
- 13 a) Y. Zhou, T. Chen, Z. Sun, S. Zhang, C. Ji, C. Song, and J. Luo, *Chem. Asian J.*, 2015, **10**, 247–251; b) Y. Tang, C. Ji, Z. Sun, S. Zhang, Chen and J. Luo, *Chem. Asian J.*, 2014, **9**, 1771 – 1776.
- 14 a) Aizu, K. *Phys. Rev. B: Solid State*, 1970, **2**, 754–772. b) T. V. Duncan, K. Song, S-T. Hung, I. Miloradovic, A. Nayak, A. Persoons, T. Verbiest, M. J. Therien and K. Clays, *Angew. Chem. Int. Ed.*, 2008, **47**, 2978-2981.
- 15 J. Zyss, J. L. Oudar, *Phys. Rev. A*1982, **26**, 2028-2048.

## Table of contents (TOC)

An Organic-Inorganic Hybrid Co-crystal Complex as High-Performance Solid-State Nonlinear Optical Switch

Tianliang Chen, Zhihua Sun,\* Sangen Zhao, Chengmin Ji and Junhua Luo\*



An organic-inorganic hybrid co-crystal complex exhibits an attractive switching nonlinear optical performance with a superior contrast and high repeatability.